Journal of Aerosol Science 69 (2014) 150–159

Contents lists available at ScienceDirect

Journal of Aerosol Science

journal homepage: www.elsevier.com/locate/jaerosci

Calibration of the new electrical low pressure impactor (ELPI+)

A. Järvinen*, M. Aitomaa, A. Rostedt, J. Keskinen, J. Yli-Ojanperä

Tampere University of Technology, Department of Physics, Aerosol Physics Laboratory, P.O. Box 692, FI-33101 Tampere, Finland

ARTICLE INFO

Article history:
Received 12 September 2013
Received in revised form
2 December 2013
Accepted 9 December 2013
Available online 18 December 2013

Keywords:
Electrical Low Pressure Impactor
ELPI+
Impactor
Charger

ABSTRACT

A renewed Electrical Low Pressure Impactor (ELPI+) was introduced by Dekati Ltd. in late 2010. This study presents the collection efficiencies of the ELPI+ cascade impactor stages and the back-up filter as well as the charging efficiency of the corona charger in the size range of 0.01–10 μm. According to the measurements the impactor cut diameters are within ±10% to the predecessor except the upmost stage for which the difference was found to be −18%. The secondary collection of nanoparticles was found to be similar to the predecessor for stages with the largest cut diameters but higher for the stages with the smallest cut diameters. The charging efficiency is higher for the new charger compared to the old one by 54% at 20 nm particle size. This study also presents the first use of the Single Charged Aerosol Reference (SCAR) for impactor and charger calibrations.

1. Introduction

Cascade impactors are widely applied for aerosol particle measurements. Numerous impactors have been designed, manufactured, and applied for aerosol studies (Marple, 2004). The Electrical Low Pressure Impactor (ELPI) enabled real-time detection of particles by combining electrical detection of charged particles with a 12-stage low pressure cascade impactor (Keskinen et al., 1992; Marjamäki et al., 2000). The ELPI has been manufactured and distributed by Dekati Ltd. since 1995. It has become a widely used instrument for air quality (Gouriou et al., 2004), combustion aerosol (Yi et al., 2008; Coudray et al., 2009) and engine exhaust measurements (Shi et al., 1999; Maricq et al., 2000; Zervas et al., 2005). It has also been applied to pharmaceutical inhaler development (Glower & Chan, 2004), as well as to atmospheric aerosol research (Held et al., 2008; Virtanen et al., 2010).

Along with time, the measuring particle size range of the ELPI has been extended towards smaller nanoparticles. Marjamäki et al. (2002) introduced a filter stage in order to detect particles smaller than 30 nm, which was the cut diameter of the lowest impactor stage at that time. In addition, an extra stage with a design cut diameter of 17 nm was developed by Yli-Ojanperä et al. (2010a). The extra stage was demonstrated to improve the nanoparticle resolution of the ELPI, but it has not been commercially available. Owing to the fixed dimensions of the impactor assembly, two uppermost stages had to be removed in order to make use of both the filter stage and the extra stage at the same time.

In 2010 Dekati Ltd. introduced a new instrument version called ELPI+, in which the impactor assembly was realized so that all the designed stages, including the 17 nm extra stage, can be used simultaneously. This increased the total number of stages to 15, including 14 impactor stages (contains one precut stage, not measured electrically) plus a filter stage. This allows real-time measurements of particle size distributions in wide particle size range from 6 nm to 10 μm according to manufacturer with 14 particle size fractions. The appearance is changed moderately from the previous model, including modification of the impactor stages. The new instrument can also be used as stand-alone, thus PC connection is not required

* Corresponding author. Tel.: +358 40 198 1024.
E-mail address: anssi.jarvinen@tut.fi (A. Järvinen).

0021-8502/$ - see front matter © 2013 Elsevier Ltd. All rights reserved.
http://dx.doi.org/10.1016/j.jaerosci.2013.12.006

but can be used. The electrometers have been redesigned and a sampling rate of 10 Hz can now be achieved. The unipolar corona charger is completely new. The most significant modification to the previous model is the smaller inner volumes of the charger and the impactor. The smaller volumes are motivated by decreased instrument size and mass, improved time response, and by smaller space charge losses at high concentrations.

The calibrations are the subject of this study. Both the charger efficiency and the impactor collection efficiency functions were measured over the operating particle size range of the instrument. The collection efficiency of the new filter stage was measured using nanoparticles. In addition to the cutpoints, all the other impactor stage parameters that are required in order to apply inversion algorithms (e.g. Lemmetty et al., 2005) and to estimate the effective density of the particles (Ahlvik et al., 1998; Maricq et al., 2000; Ristimäki et al., 2002) were evaluated. All of the calibration results and associated uncertainty values, as well as the calibration setups are presented in this paper. All measurements were conducted using monodisperse di-octyl sebacate (DOS) particles generated either with an Evaporation Condensation Generator (ECG), a Vibrating Orifice Aerosol Generator (VOAG) or with the recently introduced Single Charged Aerosol Reference (SCAR, Yli-Ojanperä et al., 2010b).

2. ELPI+ instrument

The particle measurement method of the ELPI+ has been introduced by Keskinen et al. (1992) and is based on unipolar charging of particles, size classification of these particles in cascade impactor and electrical measurement of collected particles. The operating principle and main components of the ELPI+ are presented in Fig. 1.

The aerosol is introduced into a unipolar diffusion charger which is based on needle type corona discharge. The discharge is achieved by positive high voltage of approximately 3.5 kV. In order to achieve stable charging conditions, the discharge current is kept at a constant value of 1 μA. Both discharge current and voltage are monitored by the electronics for diagnostic purposes. In the following stage the remaining ions from the corona discharge are removed from the flow by an ion trap. In the ion trap aerosol flows between two concentric cones with a potential difference of 20 V, resulting in an electric field which removes the ions from the flow.

The size classification occurs in the cascade impactor. The first stage is used as a pre-separator to remove large particles. The following 13 impactor stages are separated from each other by electrical insulators and connected to a multichannel electrometer. The unipolarly charged particles depositing on the stages are detected by measuring electric current from each stage. The last impactor stage is based on design by Yli-Ojanperä et al. (2010a). The final stage is the filter collecting the particles which are too small to be deposited by impaction in the previous stages. The filter stage is connected to the electrometer as the impactor stages. The downstream pressure is measured and can be set to the manufacturer specified value of 40 mbar by adjusting a control valve, situated between the filter stage and the connection to external vacuum. In addition to downstream pressure also the absolute pressure in the charger is measured by the electronics.

The ELPI+ is equipped with a pump which provides filtered particle free air into the charger region when the flush mode is activated. This enables zero check and adjustment of the electrometer zero levels. The electrometers are bipolar allowing particle charge studies when the diffusion charger is switched off. The operation of the instrument is controlled by an internal computer and as already mentioned, the instrument can be used as a stand-alone unit.

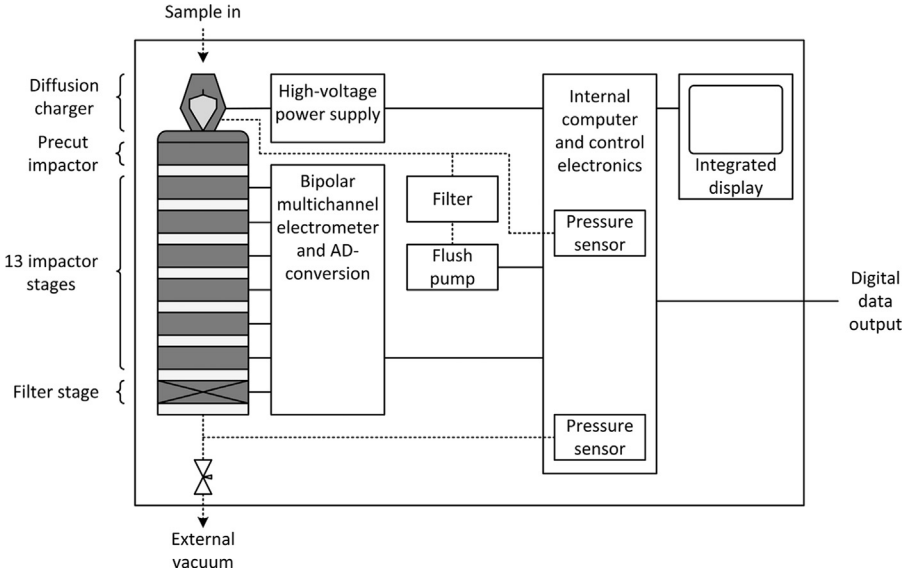

Fig. 1. The schematics of the ELPI+.

3. Impactor and charger calibration

An electrical calibration method for impactors was presented by Hillamo and Kauppinen (1991) and modified by Keskinen et al. (1999) for the cascade impactors. Fraction of the particles collected by each stage is calculated from the measured electric current values. Provided that the input particle size distribution is monodisperse and particles are unipolarly charged, the collection efficiency for stage n, is calculated based on the following equation:

$$E_n = \frac{I_n}{\sum_{i=1}^{n} I_i}, \tag{1}$$

where I_i is the current measured from the stage i ($i=1$ for the filter stage). This equation is used to estimate the secondary collection of fine particles onto the impactor stages as well (Virtanen et al., 2001). The collection efficiency of the filter stage is measured using two identical electrically insulated filters on top of each other. By assuming that the collection efficiencies of both filters are the same, the collection efficiency becomes

$$E_1 = 1 - \frac{I_{F2}}{I_{F1}}, \tag{2}$$

where I_{F1} is the current measured from the first filter stage and I_{F2} is the current measured from the filter stage located last in the flow direction. Based on the experimental collection efficiency curves, cutpoints of the stages and the steepness of the curves are obtained using the following fit function for the calibration data (Dzubay & Hasan, 1990; Winklmayr et al., 1990)

$$E_n = \left[1 + \left(\frac{d_{50}}{d_a}\right)^{2s}\right]^{-1}, \tag{3}$$

where d_a is the aerodynamic particle diameter, d_{50} the cutpoint and s describes the steepness of the collection efficiency curve. In addition to the cutpoints, the corresponding Stokes numbers (Stk_{50}) are calculated as

$$Stk_{50} = \frac{\rho_p U C(d_{50}) d_{50}^2}{9\eta W}, \tag{4}$$

where ρ_p is the particle density, U is the average jet velocity in the impactor nozzle exit calculated according to Hering (1987), η is the dynamic viscosity of gas, W is the jet diameter at the nozzle and $C(d_{50})$ is the slip correction factor at the stage inlet stagnation conditions.

The electric currents measured by the ELPI+ electrometers depend on the performance of the charger. In order to calculate the particle concentration for each impactor stage, the charging efficiency has to be known as a function of particle size. Typically, it is represented as a product of penetration P and the average number of elementary charges per particle n as follows:

$$Pn = \frac{I}{NeQ}. \tag{5}$$

In Eq. (5), I is the measured electric current after the charger which is generated by the flow of charged particles, N is the particle number concentration, e is the elementary charge and Q is the flow rate through the charger (Marjamäki et al., 2000). Concentration N can be measured with a calibrated instrument which is connected in parallel with the charger.

4. Experimental

4.1. Collection efficiency measurements

Monodisperse particles were generated using three different methods. In addition to the conventional means of Evaporation Condensation Generator (ECG) and Vibrating Orifice Aerosol Generator (VOAG), a new method for generating monodisperse particles, namely the SCAR (Yli-Ojanperä et al., 2010b), was also applied. With the SCAR, originally designed to be a concentration reference, it is possible to generate truly monodisperse particles with electrical classification, since only 0.5% of the particles from SCAR outlet have more than one elementary charge at worst case (Högström et al., 2011).

The schematics of the calibration setups are presented in Fig. 2. Setup A was applied to the particles generated using the ECG and the SCAR in the size range of 0.01–1 μm. Both methods were based on the same setup A except the particle generation was different. In the ECG method dioctyl sebacate (DOS) was first nebulized, then evaporated in a heated glass tube and cooled rapidly leading to homogeneous nucleation. The particle size was controlled by regulating the evaporation and cooling temperatures and DOS droplet concentration. The formed particles were charged by a ^{85}Kr aerosol neutralizer.

In the SCAR method 10–12 nm NaCl seed particles were generated in a tube furnace (Yli-Ojanperä et al., 2010b). Particles were charged by a ^{85}Kr-neutralizer and classified using a differential mobility analyzer, DMA (Model 3085, TSI Inc.). These singly charged particles were then introduced to a saturator where DOS is evaporated. When this DOS rich aerosol is cooled,

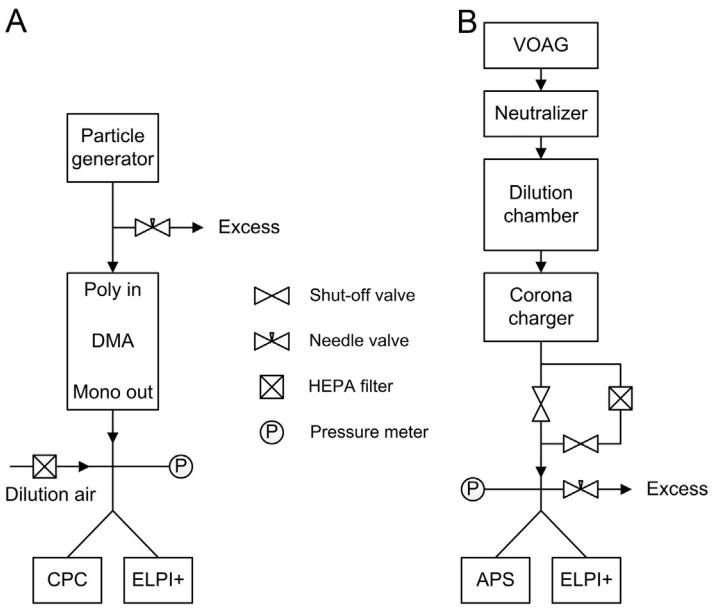

Fig. 2. ELPI+ calibration setup in case of (A) ECG, SCAR and (B) VOAG.

the vapor condenses on the charged seed particles resulting in larger particles, each with a single elementary charge. The size was controlled mainly by regulating the saturator temperature of the SCAR.

The charged aerosol generated either by the ECG or the SCAR method was introduced to a calibrated DMA (Models 3071 and 3085, TSI Inc.) to select monodisperse particles. In case of ECG, the DMA voltage was adjusted to classify particles larger than the peak size of the distribution to reduce the effect of multiple charging. In case of SCAR this was not needed as it produces particles with a single elementary charge. After the DMA aerosol was diluted with HEPA filtered air and divided between a condensation particle counter, CPC (Model 3025, TSI Inc.) and ELPI+. The CPC was only used to monitor the stability of the particle generation. The actual impactor calibration results were achieved solely by using the electrical currents measured by the ELPI+. The instrument inlet pressure was measured and adjusted to standard conditions by controlling the excess flow between the particle generator and the DMA.

The filter stage collection efficiency was measured using two identical filters on top of each other located at the bottom of the impactor assembly. The measurement setup was similar to the one presented in Fig. 2A with some differences. The particles were generated using the SCAR in the range of 10–20 nm. These particles were NaCl seed particles which were classified by the internal DMA of the SCAR allowing the second DMA to be removed.

Larger particles, sized from 1 to 10 μm were generated with a modified VOAG (Fig. 2). The vibrating piezoelectric disc of the VOAG was taken from Model 3050 (TSI Inc.), but otherwise the device comprised of a high pressure syringe pump (Nexus 6000, Chemyx Inc.), orifices with diameters of 10 and 20 μm (Lenox Laser Corp.), a signal generator (E-310B, B&K Precision) and a counter (Model 5314A, Hewlett-Packard Co.). The operation of the signal generator and counter was ensured with an oscilloscope (TDS 224, Tektronix Inc.). The particle material was DOS dissolved in 2-propanol (HPCL grade with reported evaporation residue). The droplets generated by the VOAG were introduced to a radioactive neutralizer consisting of ^{241}Am foil with an activity of 59 MBq to decrease particle losses due to electrostatic effects. After this, the droplets were brought to a dilution chamber where 2-propanol was evaporated resulting particles composing of DOS only. Particles were found to be positively charged even after the neutralization. A corona charger with negative polarity was installed after the dilution chamber to control the charge level of the aerosol for reasons discussed in Section 4.2. The aerosol was directed either straight to the instruments or through HEPA filter to provide a zero level. The inlet pressure was measured and controlled by adjusting the excess flow before the instruments. An Aerodynamic Particle Sizer (APS, Model 3321, TSI Inc.) was used in parallel with the ELPI+ to ensure the monodispersity of the generated particles. The particle diameter in each measurement point was calculated from the VOAG operating parameters according to Berglund and Liu (1973).

All collection efficiency measurements were conducted at the inlet pressure of (1013 ± 2) mbar and in typical laboratory temperature, from 19 to 24 °C. The ELPI+ downstream pressure was measured after the last impactor stage and adjusted to 40 mbar for correct operation. The sample flow rate was measured to be 10.1 lpm (Gilian Gilibrator 2, Sensidyne LP). The DMA flow rates were calibrated against a reference consisting of a combination of a calibrated laminar flow element and a differential pressure sensor (FCO332 DP, Furness Controls Ltd.). The size response of the DMA was confirmed with standard particles (Thermo Fisher Scientific Inc.).

4.2. Charging efficiency measurements

The charging efficiency was determined using monodisperse particles by measuring the total electric current from the impactor which was connected to the charger as in normal use. Particles were generated with SCAR in the size range of 0.01–1.9 μm and with VOAG in the size range of 1.5–10 μm, by using the setups shown in Fig. 2 with minor modifications.

The ELPI+ charger provides positive charge onto the particles. If the particles going into the charger are initially positively charged the output of the charger may be affected especially in the small particle sizes where the charging efficiency is low. To avoid this effect, initially negatively charged particles were used in the calibration.

In order to produce negatively charged particles using the setup A in Fig. 2, the polarities of the internal DMA of the SCAR and the following classifying DMA were changed from negative to positive (negative particle output). To be able to measure particles larger than 1 μm, the inlet and outlet tubing of the classifying DMA were modified. By applying these modifications it was possible to calibrate the ELPI+ charger using singly charged particles with a mobility diameter from 0.01 to 1.9 μm. The DMA output was diluted and connected to a static mixer (Kenics 37-06-110, Chemineer Inc.) followed by a flow splitter (Model 3708, TSI Inc.). From this flow splitter, the aerosol was introduced to the ELPI+ and to a CPC (Model 3776, TSI Inc.). The CPC was used as concentration reference in the calibration. Both the CPC counting efficiency and the size response were calibrated prior to the ELPI+ measurements using the SCAR and a Faraday-cup electrometer as a reference (see, e.g. Yli-Ojanperä et al., 2012). The charging efficiency was measured also by switching the ELPI+ charger on and off. Both methods were found to give equal results but the CPC provided more stable results with less scatter. The actual charging efficiency was calculated using Eq. (5) where the electric current was measured from the impactor by ELPI+ electrometers and the particle number concentration was measured by the CPC.

The VOAG was used in measurement of the charging efficiency from 1.5 to 10 μm for which the setup B shown in Fig. 2 was applied. To achieve reliable results the smallest VOAG particle sizes were selected to overlap with the results measured with the SCAR. In the VOAG measurements, the APS was used as a concentration reference and to ensure that the particle distribution was monodisperse. Residual particles were observed when the VOAG was operated using the solvent only. For this reason, the APS was used as particle size reference from 1.5 to 4 μm. The APS-measured aerodynamic diameter was converted into mobility diameter. In case of the largest particle size range from 2.9 to 10 μm the diameters were calculated according to the parameters used for the VOAG, again this size range had an overlap with the smaller measurement series.

In the VOAG measurements particles were initially neutralized by a radioactive neutralizer. However, the particles were observed to be still positively charged as in case of collection efficiency measurements. Thus, a study was conducted to evaluate the effect of the initial particle charge on the operation of the charger. Particles having a high positive initial charge will have higher charge state at the output than expected which leads to higher electric current and overestimation of the particle concentration. To investigate this, a test was conducted using a constant particle size of 3.2 μm. In this test initial charge was adjusted with an additional corona charger installed between the dilution chamber of the VOAG and the instruments. The measurement was conducted for both ELPI and ELPI+. An APS was used to determine the particle concentration. Together with the electrometer readings, the APS number concentration was used to calculate the elementary charges per particle ratio.

It was found that the initial negative charge on the particles does not have an effect on the efficiency of the charger which can be noticed from Fig. 3. However, an initial charge of more than 100 positive elementary charges will result in an increased charging state and error in particle concentration if it is calculated using the pre-defined *Pn*-value which is approximately 400 for 3.2 μm particles. The two different slopes in Fig. 3 correspond to measurements conducted on two separate days with the same calibration setup. The reason for this difference is unknown but may be related to electrostatic losses in the tubing.

The results of the initial charge test were applied to the measurement of the charging efficiency. To ensure reliable measurements negative corona charger was placed between the VOAG and the measuring instruments, ELPI+ and APS as in

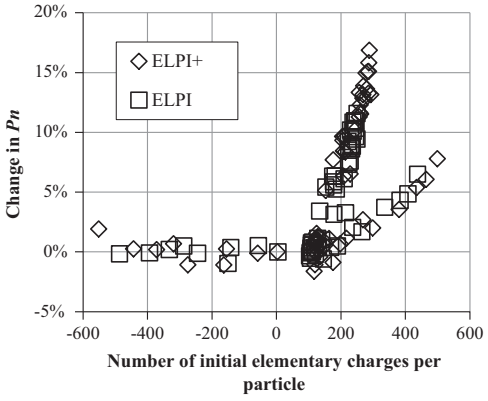

Fig. 3. The effect of particle initial charge on ELPI and ELPI+ charger output. The particle physical diameter was 3.2 μm.

case of the charge test. Particles were given a slightly negative charge which was checked before and after the measurement by switching the ELPI+ charger off.

5. Results

5.1. Impactor

The impactor calibration was conducted using monodisperse particles with well-defined mobility or physical diameter. These diameters were converted into particle aerodynamic diameter which was calculated at the inlet stagnation pressure of each impactor stage. The collection efficiencies of the ELPI impactor stages as a function of aerodynamic diameter are presented in Fig. 4 with *s*-functions fitted according to Eq. (3). The data for the multiple charged ECG generated particles was corrected up to 6 elementary charges using a method described by Kauppinen and Hillamo (1989). The measured data points determined using the SCAR and the corrected data points obtained using the ECG method were in a good agreement for stage 9, which implies that the correction algorithm works rather well. The collection efficiencies of the impactor stages having the smallest cut diameters do not reach zero towards smaller particle sizes. This effect arises from secondary collection of particles by diffusion. For the largest particles (stages 12, 13 and 14) the collection efficiency approaches unity slower than expected. In general, the measurement points having different particle generation methods overlap nicely, implying that the particle diameters are well defined for the different methods.

Cut diameters d_{50} were calculated from the fitted *s*-functions. Cut diameters, the corresponding Stokes numbers and fitted steepness values are listed in Table 1, together with the data of the previous model. However, the measurements in Marjamäki (2003) for previous ELPI were carried out at the ambient pressure of 985.4 mbar. Therefore the calibration data taken from the Marjamäki (2003) was converted to the standard inlet pressure of 1013 mbar with the conversion described by Hering (1987).

Comparison to previous model shows very similar cut sizes and Stokes numbers with the exception of the two upmost stages. Stages 13 and 14 have distinctively smaller cut sizes than the previous model. This implies that the smaller volume of the stages has in fact modified the impaction characteristics of the stages. For stage 7, where a first significant pressure drop occurs, the collection efficiency curve is much steeper. Therefore it appears that the stage works more like an ideal stage. The lowest impactor stage cut diameter 15.7 nm is close to the 16.7 nm value given by Yli-Ojanperä et al. (2010a). The collection efficiency of the new filter stage was found to be 97% for particles in the size range of 10–20 nm. In general the ELPI+ impactor cut diameters and curve steepness values are close to the values of the previous model with the additional information given by the new 15.7 nm impactor stage. In terms of nanoparticles, the new ELPI+ impactor should have better response to inversion algorithms (Lemmetty et al., 2005) and to the measurement of the effective density of the particles (Ristimäki et al., 2002) compared to the previous model because of the new 15.7 nm stage.

The uncertainties of the experimentally determined cut-points were evaluated separately for different particle generation methods. From 0.01 to 1 μm the uncertainty of the particle size is mainly caused by the sizing accuracy of the DMA. Following the uncertainty evaluation presented by Mulholland and Fernandez (1998), the uncertainties of the reported cut-points are 5% with 95% confidence interval. For larger particles the uncertainty of the particle size derives from the uncertainty of the VOAG operating parameters, including liquid concentration, feed rate, frequency, impurity concentration and doublet particles. By taking all these factors into account 2% uncertainties for the cut-points are obtained with 95% confidence interval, which is in good agreement with the values reported by Berglund and Liu (1973).

In order to calculate the true particle concentration and distribution, the secondary collection of particles in the ELPI+ needs to be known. Particle collection in impactor occurs in addition to impaction due to diffusion and electric effects: space charge and image charge. These effects have been analyzed by Virtanen et al. (2001) and Marjamäki et al. (2005). In this

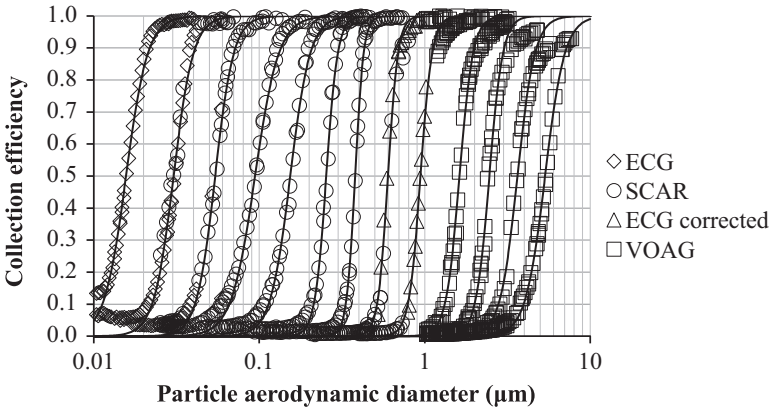

Fig. 4. Measured collection efficiency curves and fitted *s*-functions for stages 2–14. "ECG corrected" refers to results which were achieved by using the multiple charge correction algorithm.

Table 1
Cut diameters d_{50}, corresponding square roots of the Stokes numbers $\sqrt{Stk_{50}}$ and curve steepness values s for the calibrated ELPI+. The values for the previous model calibrated by Marjamäki (2003) are given for comparison.

ELPI+ stage	ELPI+			ELPI stage	ELPI		
	d_{50} (μm)	$\sqrt{Stk_{50}}$	s		d_{50} (μm)	$\sqrt{Stk_{50}}$	s
1 (Filter)	–	–	–	Filter	–	–	–
2	0.0157	0.447	3.32	–	–	–	–
3	0.0304	0.431	3.65	1	0.0289	0.421	3.41
4	0.0541	0.438	3.89	2	0.0541	0.453	4.29
5	0.0943	0.442	3.05	3	0.0905	0.439	2.94
6	0.154	0.449	3.62	4	0.153	0.448	3.10
7	0.254	0.472	6.30	5	0.260	0.477	3.58
8	0.380	0.457	8.43	6	0.380	0.456	9.27
9	0.600	0.443	7.16	7	0.617	0.450	5.87
10	0.943	0.445	6.21	8	0.921	0.445	8.77
11	1.62	0.469	5.32	9	1.59	0.461	4.88
12	2.46	0.466	5.33	10	2.43	0.451	5.59
13	3.64	0.427	4.14	11	3.98	0.465	4.53
14	5.34	0.390	3.66	12	6.53	0.483	4.50
Average		0.444				0.455	

study secondary collection of fine particles was calculated using Eq. (1) considering only total efficiency of secondary collection which occurs due to diffusion and image charge because calibration was performed in low concentration environment. A power function was fitted to the data which resulted parameters listed in Table 2. The applied power function has the form of

$$E_i(D_p) = a_i D_p^{b_i} + c_i, \tag{6}$$

where E is the secondary collection efficiency, i stands for stage number and D_p is the particle mobility diameter in μm. Fitted parameters a, b and c are defined for each stage individually. Parameters were not measured for stages 1 and 2. In case of stage 2, fine particles are being collected by the impaction mechanism and the stage 1 is the filter for which the secondary collection cannot be defined. Figure 5 presents the measured data for the ELPI+ impactor stages 8 and 14. When comparing to the secondary collection data presented by Marjamäki et al. (2005), it can be seen that the secondary collection efficiency is similar to the previous ELPI for stage 14. When the stage number and the cut diameter is decreasing higher values of secondary collection are observed for the ELPI+ than for the ELPI which is visible in the stage 8 data in Fig. 5. This effect may be explained by different construction of the impactor stages between the ELPI+ and ELPI. The differences in the secondary collection should be taken into account when measurement signals are processed into particle concentration values.

5.2. Charger

The charging efficiency of the ELPI+ charger was measured from 0.012 to 8.1 μm using the SCAR and the VOAG and by applying the Eq. (5). By combination of SCAR and a calibrated CPC, high precision results were obtained from 0.012 up to 1.9 μm. For larger particle sizes, the VOAG and the APS as a reference were used. Ranges of these two different methods were selected to overlap slightly. It was found out that charger efficiencies were not identical in the overlapping section. This is attributed to a non-ideal counting efficiency of the APS. The VOAG+APS results were reduced by 16% to match the charging efficiencies obtained with the SCAR. The charger response measurement results are presented in Fig. 6 as a penetration multiplied by the average number of charges Pn as a function of particle mobility diameter.

The overall charging efficiency was found to be higher than for the previous model. This can be explained by the smaller volume of the new charger and differences in the flow patterns through the charger. A power function fitted to the data in Fig. 6 in three particle size ranges was derived as

$$Pn = \begin{cases} 68.531 D_p^{1.225}, & D_p < 1.035\ \mu\text{m} \\ 67.833 D_p^{1.515}, & 1.035\ \mu\text{m} \le D_p \le 4.282\ \mu\text{m} \\ 126.83 D_p^{1.085}, & D_p > 4.282\ \mu\text{m} \end{cases}, \tag{7}$$

where D_p is the particle mobility diameter in μm. The charging efficiency Pn is rather well described by the power functions although there is a noticeable step toward higher charging efficiencies when the particle size is increasing from 1 to 4 μm. In the smaller particle sizes the diffusion charging is the prevailing mechanism and the step may be a result of increased field charging. For particle size larger than 4 μm the charging efficiency slope (in log–log scale) is decreasing which may be due to particle losses in the charger or due to measurement errors. The latter could be caused by a number concentration

Table 2
Fitted power function parameters for the secondary collection efficiency of the ELPI+ stages.

ELPI+stage	a_i	b_i	c_i
3	9.80×10^{-8}	−2.73	0.05085
4	3.63×10^{-8}	−3.06	0.03083
5	1.58×10^{-6}	−2.26	0.02342
6	4.83×10^{-6}	−2.06	0.02183
7	1.02×10^{-5}	−1.90	0.02097
8	6.22×10^{-5}	−1.49	0.01158
9	4.03×10^{-5}	−1.56	0.00804
10	7.31×10^{-5}	−1.40	0.00671
11	1.01×10^{-4}	−1.31	0.00475
12	8.22×10^{-5}	−1.35	0.00288
13	1.09×10^{-4}	−1.31	0.00129
14	9.07×10^{-5}	−1.36	0.00186

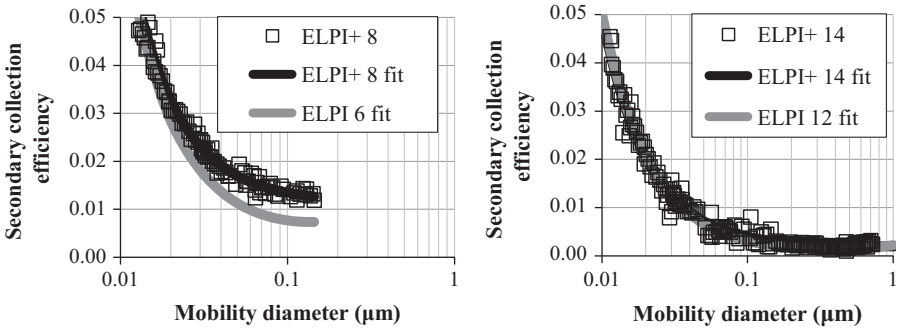

Fig. 5. Secondary collection efficiency of ELPI+ and ELPI impactors for two corresponding stages presented as a function of particle mobility diameter (ELPI fit taken from Marjamäki et al., 2005).

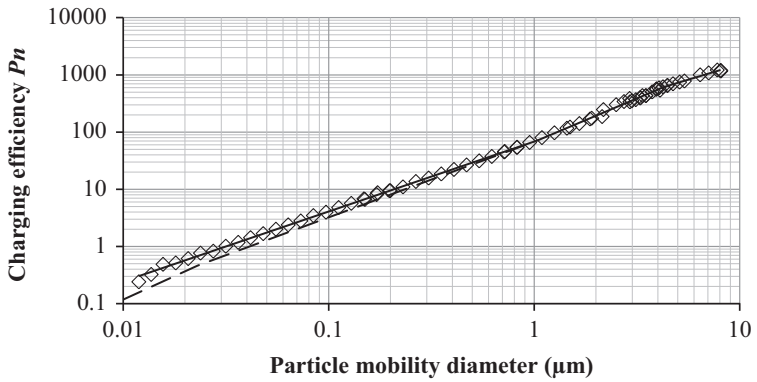

Fig. 6. ELPI+ charger efficiency *Pn*, measurement points and fitted 3-part power function. The ELPI charging efficiency by Marjamäki et al. (2002) is shown as reference (dashed line).

difference between the ELPI+ inlet and the reference inlet. Another source of error is the lack of traceable number concentration reference in this size range.

The uncertainty related to the use of the *Pn* fit-functions presented in Eq. (7) was evaluated in the size range of 0.01–2 μm. For particle sizes larger than 2 μm, no uncertainty evaluation was conducted, because of the lack of reliable number concentration references in this size range. The uncertainty consists of two components. These are the deviation of the values calculated using Eq. (7) from the experimental values and the uncertainty of the experimentally determined *Pn* values. For the deviation part, the uncertainty was estimated to be equal to two times the standard deviation of the relative difference between the experimentally determined and calculated *Pn* values. This resulted in 10.8% uncertainty with 95% confidence interval. The second uncertainty component was derived from Eq. (5) by applying the law of propagation of the uncertainty. Following uncertainty values were used in the calculation: 1% ± 1 fA for the electric current, 3% for the particle concentration, and 1% for the flow measurement. These are all based on the calibrations of the instruments. By combining

the uncertainty components (deviation and accuracy of the experimental *Pn* values) by root of the sum of squares method, size dependent uncertainty values were obtained. For the smallest particle size, the overall uncertainty is 20% (95% confidence interval), which decreases towards larger sizes and levels at 40 nm particle diameter to 12%.

6. Discussion

In this study the new Electrical Low Pressure Impactor ELPI+ was calibrated in laboratory environment. Results were in good agreement with the previous model of the ELPI for most of the impactor stages, but two upmost stages had significantly smaller cut sizes. Also the collection efficiency curve for the 7th stage was much steeper in the ELPI+. The filter stage collection efficiency was tested with nanosized particles and it was found to be approximately 97%. The secondary collection of fine particles was found to be similar to the previous model in case of the stages with the largest cut diameters. The efficiency of secondary collection was found be larger in ELPI+ in comparison to ELPI for stages with smaller cut diameters. The largest detectable particle size of the ELPI+ is a bit lower than for the previous model, but the overall particle size resolution is better since all the designed 14 impactor stages and the filter stage can now be used together in the impactor assembly. For the previous model, the two upmost stages had to be removed for the installation of the later on developed non-commercial nanoparticle stage and the filter stage. The ELPI+ impactor characteristics are close to the predecessor model allowing inversion method (Lemmetty et al., 2005) and density measurement algorithm (Ristimäki et al., 2002) to be applied to the ELPI+ data with only minor modification of the calculation parameters. The included nanoparticle stage allows these methods to be applied to smaller particle sizes with higher precision.

The new ELPI+ charger was found to be more efficient than the previous model and a new fit was derived for the conversion of measured current signal into particle number concentration. However, a study should be made to investigate the effect of particle concentration on the ELPI and ELPI+ charger's efficiency. It was found that particle initial charge has an effect on the charger output which could be studied in more detail.

It was found out that the SCAR and electrical classifying can be applied in calibrations from 10 nm up to 1.9 μm particle size allowing straightforward and accurate measurements. Above this size calibration was found to be a challenge because lack of a reliable references and possible non-uniform distribution of the particles between the instrument being calibrated and the reference. The reference issue might be solved by constructing a longer DMA cylinder in the future which would allow the SCAR to be used for even larger particle sizes.

Acknowledgments

The authors would like to acknowledge Dekati Ltd. for providing instruments to the study. This work was funded by CLEEN Ltd., the Cluster for Energy and Environment through the Measurement, Monitoring and Environmental Assessment (MMEA) research program.

References

Ahlvik, P., Ntziachristos, L., Keskinen, J., & Virtanen, A. (1998). Real Time Measurements of Diesel Particle Size Distributions with an Electrical Low Pressure Impactor. SAE Technical Paper Series 980410.

Berglund, R.N., & Liu, B.Y. H. (1973). Generation of monodisperse aerosol standards. *Environmental Science and Technology*, *7*, 147–153.

Coudray, N., Dieterien, A., Roth, E., & Trouvé, G. (2009). Density measurement of fine aerosol fractions from wood combustion sources using ELPI distributions and image processing techniques. *Fuel*, *88*, 947–954.

Dzubay, T.G., & Hasan, H. (1990). Fitting multimodal lognormal size distributions to cascade impactor data. *Aerosol Science and Technology*, *13*, 144–150.

Glower, W., & Chan, H.-K. (2004). Electrostatic charge characterization of pharmaceutical aerosols using electrical low-pressure impaction (ELPI). *Journal of Aerosol Science*, *36*(6), 755–764.

Gouriou, F., Morin, J-P., & Weill, M.-E. (2004). On-road measurements of particle number concentrations and size distributions in urban and tunnel environments. *Atmospheric Environment*, *38*, 2831–2840.

Held, A., Zerrath, A., McKeon, A., Fehrenbach, T., Niessner, R., Plass-Dülmer, C., Kaminski, U., Berresheim, H., & Pöschl, U. (2008). Aerosol size distributions measured in urban, rural and high-alpine air with an electrical low pressure impactor (ELPI). *Atmospheric Environment*, *42*, 8502–8512.

Hering, S.V. (1987). Calibration of the QCM impactor for stratospheric sampling. *Aerosol Science and Technology*, *7*, 257–274.

Hillamo, R.E., & Kauppinen, E.I. (1991). On the performance of the Berner low pressure impactor. *Aerosol Science and Technology*, *14*, 33–47.

Högström, R., Yli-Ojanperä, J., Rostedt, A., Iisakka, I., Mäkelä, J.M., Heinonen, M., & Keskinen, J. (2011). Validating the Single Charged Aerosol Reference (SCAR) as a traceable particle number concentration standard for 10 nm to 500 nm aerosol particles. *Metrologia*, *48*, 1–11.

Kauppinen, E.I., & Hillamo, R.E. (1989). Modification of the University of Washington Mark 5 in-stack impactor. *Journal of Aerosol Science*, *20*, 813–827.

Keskinen, J., Marjamäki, M., Virtanen, A., Mäkelä, T., & Hillamo, R. (1999). Electrical calibration method for cascade impactors. *Journal of Aerosol Science*, *30*, 111–116.

Keskinen, J., Pietarinen, K., & Lehtimäki, M. (1992). Electrical low pressure impactor. *Journal of Aerosol Science*, *23*, 353–360.

Lemmetty, M., Marjamäki, M., & Keskinen, J. (2005). The ELPI response and data reduction II: properties of kernels and data inversion. *Aerosol Science and Technology*, *39*, 583–595.

Maricq, M.M., Podsiadlik, D.H., & Chase, R.E. (2000). Size distributions of motor vehicle exhaust PM: a comparison between ELPI and SMPS measurements. *Aerosol Science and Technology*, *33*, 239–260.

Marjamäki, M. (2003). Electrical low pressure impactor: modifications and particle collection characteristics (Ph.D. dissertation). Tampere University of Technology, Tampere, Publication 449.

Marjamäki, M., Keskinen, J., Chen, D-R., & Pui, D.Y. H. (2000). Performance evaluation of the electrical low-pressure impactor (ELPI). *Journal of Aerosol Science*, *31*, 249–261.

Marjamäki, M., Lemmetty, M., & Keskinen, J. (2005). ELPI response and data reduction I: response functions. *Aerosol Science and Technology*, *39*, 575–582.

Marjamäki, M., Ntziachristos, L., Virtanen, A., Ristimäki, J., Keskinen, J., Moisio, M., Palonen, M., & Lappi, M. (2002). Electrical Filter Stage for the ELPI. SAE Technical Paper Series, 2002-01-0055.
Marple, V.A. (2004). History of impactors—the first 110 years. *Aerosol Science and Technology*, *38*, 247–292.
Mulholland, G., & Fernandez, M. (1998). Accurate size measurement of monosize calibration spheres by differential mobility analysis. *AIP Conference Proceedings*, *449*, 819–823.
Ristimäki, J., Virtanen, A., Marjamäki, M., Rostedt, A., & Keskinen, J. (2002). On-line measurement of size distribution and effective density of submicron aerosol particles. *Journal of Aerosol Science*, *33*, 1541–1557.
Shi, J.P., Harrison, R.M., & Brear, F. (1999). Particle size distribution from a modern heavy duty diesel engine. *The Science of the Total Environment*, *235*, 305–317.
Virtanen, A., Joutsensaari, J., Koop, T., Kannosto, J., Yli-Pirilä, P., Leskinen, J., Mäkelä, J.M., Holopainen, J.K., Pöschl, U., Kulmala, M., Worsnop, D.R., & Laaksonen, A. (2010). An amorphous solid state of biogenic secondary organic aerosol particles. *Nature*, *476*, 824–827.
Virtanen, A., Marjamäki, M., Ristimäki, J., & Keskinen, J. (2001). Fine particle losses in electrical low-pressure impactor. *Journal of Aerosol Science*, *32*, 389–401.
Winklmayr, W., Wang, H-C., & John, W. (1990). Adaptation of the Twomey Algorithm to the inversion of cascade impactor data. *Aerosol Science and Technology*, *13*, 322–331.
Yi, H., Hao, J., Duon, L., Tang, X., Ning, P., & Li, X. (2008). Fine particle and trace element emissions from an anthracite coal-fired power plant equipped with a bag-house in China. *Fuel*, *87*, 2050–2057.
Yli-Ojanperä, J., Kannosto, J., Marjamäki, M., & Keskinen, J. (2010a). Improving the nanoparticle resolution of the ELPI. *Aerosol and Air Quality Research*, *10*, 360–366.
Yli-Ojanperä, J., Mäkelä, J.M., Marjamäki, M., Rostedt, A., & Keskinen, J. (2010b). Towards traceable particle number concentration standard: Single Charged Aerosol Reference (SCAR). *Journal of Aerosol Science*, *41*, 719–728.
Yli-Ojanperä, J., Sakurai, H., Iida, K., Mäkelä, J.M., Ehara, K., & Keskinen, J. (2012). Comparison of three particle number concentration calibration standards through calibration of a single CPC in a wide particle size range. *Aerosol Science and Technology*, *46*, 1163–1173.
Zervas, E., Dorlhène, P., Forti, L., Perrin, C., Momique, J.C., Monier, R., Ing, H., & Lopez, B. (2005). Interlaboratory test of exhaust PM using ELPI. *Aerosol Science and Technology*, *39*, 333–346.